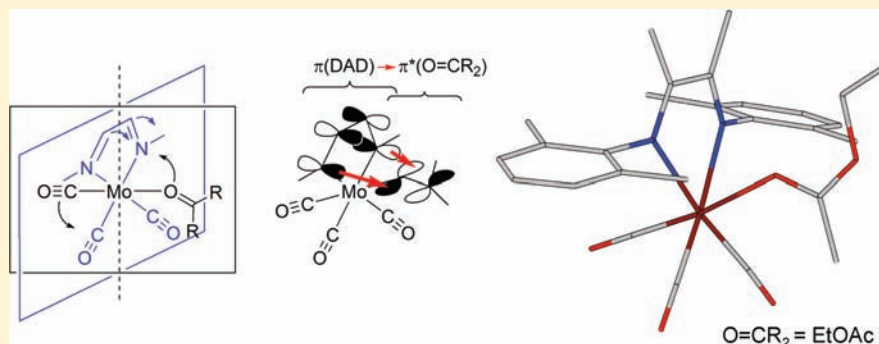


Molybdenum 1,4-Diazabuta-1,3-diene Tricarbonyl Solvento Complexes Revisited: From Solvatochromism to Attractive Ligand–Ligand Interaction

Benjamin Oelkers, Alexander Venker, and Jörg Sundermeyer*

Fachbereich Chemie, Philipps-Universität Marburg, Hans-Meerwein-Straße, 35032 Marburg, Germany

S Supporting Information



ABSTRACT: Various complexes of the types $[\text{Mo}(\text{DAD})(\text{CO})_3\text{L}]$ ($\text{L} = \text{CO}, \text{MeCN}, \text{MeOH}, \text{THF}, \text{DMSO}, \text{DMF}, \text{Me}_2\text{CO}, \text{EtOAc}, \text{THT}, \text{Im}^{\text{H}}, \text{Im}^{\text{I}}, t\text{BuNC}, n\text{Bu}_3\text{P}$), $(\text{ER}_4)[\text{Mo}(\text{DAD})(\text{CO})_3\text{X}]$ ($\text{ER}_4 = \text{NEt}_4^+$; $\text{X}^- = \text{Cl}^-, \text{Br}^-, \text{I}^-, \text{NCS}^-, \text{CN}^-$ and $\text{ER}_4^+ = \text{PPh}_4^+$; $\text{X}^- = \text{N}_3^-$), and $(\text{ER}_4)[\{\text{Mo}(\text{DAD})(\text{CO})_3\}_2(\mu\text{-X})]$ ($\text{ER}_4^+ = \text{NEt}_4^+$; $\text{X}^- = \text{CN}^-, \text{OAc}^-$ and $\text{ER}_4^+ = \text{PPh}_4^+$; $\text{X}^- = \text{N}_3^-$; $\text{DAD} = N,N'$ -bis(2,6-dimethylphenyl)butane-2,3-diimine) were prepared by ligand exchange from cycloheptatriene molybdenum tricarbonyl. A total of 19 crystal structures were determined, including unprecedented structural characterization of molybdenum(0) coordination by dimethyl sulfoxide (DMSO), methanol, ethyl acetate (EtOAc), acetone, and N,N -dimethylformamide (DMF). Correlation of ^{13}C NMR shifts with the complex geometry suggests a direct ligand–ligand interaction between DAD and O-bonded coligands with $\text{C}=\text{O}$ and $\text{S}=\text{O}$ double bonds, such as EtOAc, Me_2CO , DMF, and DMSO. Unexpectedly, the solvatochromic properties of these tricarbonyl complexes $[\text{Mo}(\text{DAD})(\text{CO})_3\text{L}]$ are unfavorable for the determination of Kamlet–Taft parameters of the corresponding solvent L . Contrastingly, the UV/vis absorption of $[\text{Mo}(\text{DAD})(\text{CO})_4]$ is strongly correlated with the Kamlet–Taft parameter π^* , which is shown for 22 solvents, including seven room temperature ionic liquids.

INTRODUCTION

Carbonyl complexes of zerovalent group VI metals, especially of molybdenum, bearing unsaturated diaza ligands are one of the most studied compound classes since the early days of organometallic chemistry. Mainly, the tetracarbonyl complexes $[\text{Mo}(\text{N}-\text{N})(\text{CO})_4]$ have attracted a lot of interest concerning all four major types of planar 1,4-diaza ligands (N–N), i.e., 1,4-diazabutadienes (DAD),¹ bipyridines (bipy),^{1h,2} phenanthrolines (phen),^{2m,3} and iminopyridines (pyridine-2-carbaldimines, PyCa).^{1h,4} Among the most interesting features of these complexes are characteristic metal–ligand charge-transfer (MLCT) bands that show strong solvatochromic behavior^{1c,4b,5} and have thus been used for the empirical determination of the solvent polarity.^{5a,6} Further studies include photoexcitation,⁷ multimetallic complexes,⁸ electrochemistry,⁹ and polymerization of methyl methacrylate.¹⁰

Formal substitution of one carbonyl ligand by a neutral (L) or anionic coligand (X^-) leads to tricarbonyl complexes $[\text{Mo}(\text{N}-\text{N})(\text{CO})_3(\text{L}/\text{X})]^{0/-}$ that are found to be *fac*-configured for all but the most π -accepting coligands, which is due to the pronounced trans effect of CO. While considerable work has been

done concerning phen and bipy complexes, especially covering strong donor/acceptor ligands,^{1h,11} (weakly) donating solvents,^{9f,12} and (pseudo)halide anions,¹³ less is known for DAD-based complexes. Only neutral coligands with large ligand-field splitting (P-based ligands,^{1d,f,2d,5b,6a,7c,d,14} isonitriles,¹⁵ cyclooctene,¹⁶ and acetonitrile^{1f,14a,b,15b}) have been applied in this case (tables listing all known tricarbonyl complex preparations and crystal structures are given in the Supporting Information, SI).

In contrast to a plethora of X-ray diffraction (XRD) studies on tetracarbonyl complexes $[\text{Mo}(\text{N}-\text{N})(\text{CO})_4]$, surprisingly little structural information is available in the literature on the corresponding tricarbonyl complexes $[\text{Mo}(\text{N}-\text{N})(\text{CO})_3\text{L}]$, being limited to phosphanes,¹⁷ pyridine,¹⁸ isonitriles,^{17b,19} tetrahydrofuran (THF),^{17b} and sulfur dioxide.²⁰ No complexes of the type $[\text{Mo}(\text{N}-\text{N})(\text{CO})_3\text{X}]^-$ have been structurally characterized; this also holds for molybdenum 1,4-diazabuta-1,3-diene tricarbonyl complexes with any coligand. Concerning (weak) donor solvents

Received: November 22, 2011

Published: March 28, 2012

like amides, carboxylates, ketones, alcohols, dimethyl sulfoxide (DMSO), or tetrahydrothiophene (THT), little to no structural information is available for molybdenum(0) complexes of any kind.

Because the tricarbonyl complexes $[\text{Mo}(\text{N}-\text{N})(\text{CO})_3(\text{L}/\text{X})]^{0/-}$ are known to easily exchange the monodentate coligand (L/X⁻) in equilibrium reactions,^{12a,13a,14a,b} we decided to investigate whether the corresponding, up to now unknown, DAD complexes are accessible. If so, the complex fragment $[\text{Mo}(\text{DAD})(\text{CO})_3]$ could serve as a spectroscopic tool for solvent-polarity measurements with behavior presumably different from that of the corresponding tetracarbonyl complex $[\text{Mo}(\text{DAD})(\text{CO})_4]$ (**1**).²¹ The latter was also tested for comparison, including the first reported use of such chromophores for the solvatochromic description of ionic liquids (ILs). NMR spectra and solid-state structures could be obtained for most compounds and provide a reliable basis on which the observed UV/vis spectra will be discussed.

DAD ligands are easily tunable because of their facile preparation from various α -diketones and primary amines. In order to get a consistent data set, only one member of this ligand family was used throughout our study, namely, *N,N'*-bis(2,6-dimethylphenyl)butane-2,3-diimine, which will in the following be abbreviated to DAD.

EXPERIMENTAL SECTION

Synthesis of Compounds. Preparation and characterization data are given for one example of each synthetic protocol applied. Full experimental details for all compounds are given in the SI.

$[\text{Mo}(\text{DAD})(\text{CO})_3(\text{DMSO})]$ (**5**; *Method A*). A mixture of $[\text{Mo}(\text{C}_7\text{H}_8)(\text{CO})_3]$ (288 mg, 1.06 mmol, 1.03 equiv) and DAD (302 mg, 1.03 mmol, 1.00 equiv) was dissolved in toluene (15 mL). DMSO (0.1 mL, 1.3 mmol, 1.3 equiv) was added, resulting in a dark-blue reaction mixture. After stirring overnight, the precipitated product was isolated by filtration and dried in vacuo. Yield: 506 mg (89%), microcrystalline, violet-blue powder. ¹H NMR (300 MHz, CD₂Cl₂): δ 1.99 (s, 6H, CH₃), 2.18 (s, 12H, CH₃), 2.65 (s, 6H, (CH₃)₂SO), 7.06–7.17 (m, 6H, C_{arom}H). ¹³C NMR (75 MHz, CD₂Cl₂): δ 18.5, 18.9, 19.5 (CH₃), 39.3 ((CH₃)₂SO), 125.6, 128.5, 128.6, 128.9, 150.0 (C_{arom}), 169.9 (C=N). IR (neat): ν 2920 (w), 1890 (s), 1781 (s), 1754 (vs), 1602 (w), 1517 (w), 1465 (m), 1421 (w), 1375 (w), 1308 (m), 1258 (w), 1215 (m), 1095 (w), 1021 (w), 990 (m), 956 (w), 940 (m), 846 (w), 769 (m), 699 (w), 640 (w), 626 (w), 507 (w), 425 (w) cm⁻¹.

$[\text{Mo}(\text{DAD})(\text{CO})_3(\text{DMF})]$ (**6**) and $[\text{Mo}(\text{DAD})(\text{CO})_3(\text{THT})]$ (**9**) were obtained using the same protocol; see the SI.

$[\text{Mo}(\text{DAD})(\text{CO})_3(\text{MeCN})]$ (**2**; *Method B*). To a mixture of $[\text{Mo}(\text{C}_7\text{H}_8)(\text{CO})_3]$ (825 mg, 3.03 mmol, 1.00 equiv) and DAD (885 mg, 3.03 mmol, 1.00 equiv) was added acetonitrile (30 mL). The dark-blue reaction mixture was stirred overnight. Afterward, the precipitated product was isolated by filtration and dried in vacuo. Yield: 1276 mg (82%), microcrystalline, dark-blue powder. ¹H NMR (300 MHz, CD₂Cl₂): δ 2.00, 2.09 (2 \times s, 2 \times 6H, CH₃), 2.17 (s, 3H, CH₃CN), 2.21 (s, 6H, CH₃), 7.07–7.19 (m, 6H, C_{arom}H). ¹³C NMR (75 MHz, CD₂Cl₂): δ 3.9 (CH₃CN), 18.2, 19.0, 19.4 (CH₃), 125.6, 128.3, 128.5, 128.7, 129.1, 150.7 (C_{arom}), 167.8 (C=N). ¹H NMR (300 MHz, CD₃CN): δ 1.96 (s, 3H, CH₃CN), 2.02, 2.14, 2.23 (3 \times s, 3 \times 6H, CH₃), 7.06–7.20 (m, 6H, C_{arom}H). ¹³C NMR (75 MHz, CD₃CN): δ 1.8 (CH₃CN), 18.3, 19.3, 19.8 (CH₃), 126.3, 128.5, 129.4, 129.5, 151.0 (C_{arom}), 171.5 (C=N). IR (neat): ν 2978 (w), 2920 (w), 1903 (s), 1826 (sh), 1812 (s), 1776 (vs), 1555 (w), 1462 (m), 1433 (m), 1409 (m), 1376 (m), 1307 (s), 1257 (w), 1216 (m), 1164 (w), 1092 (w), 1032 (w), 971 (m), 847 (m), 774 (m), 700 (m), 635 (m), 558 (w), 529 (w), 510 (m), 477 (w), 434 (m) cm⁻¹.

$[\text{Mo}(\text{DAD})(\text{CO})_3(\text{MeOH})] \cdot 3\text{MeOH}$ (3·3MeOH), $[\text{Mo}(\text{DAD})(\text{CO})_3(\text{Me}_2\text{CO})]$ (**7**), and $[\text{Mo}(\text{DAD})(\text{CO})_3(\text{EtOAc})]$ (**8**) were obtained according to the same protocol; see the SI.

$(\text{NEt}_4)[\text{Mo}(\text{DAD})(\text{CO})_3\text{Cl}]$ (**14**; *Method C*). A mixture of $[\text{Mo}(\text{C}_7\text{H}_8)(\text{CO})_3]$ (278 mg, 1.02 mmol, 1.00 equiv), DAD (298 mg, 1.02 mmol, 1.00 equiv), and NEt₄Cl (202 mg, 1.21 mmol, 1.19 equiv) was dissolved in dichloromethane (15 mL). The dark-blue reaction mixture was stirred

for 60 min. Afterward, the product was precipitated by the addition of hexane (25 mL), isolated by filtration, and dried in vacuo. Yield: 412 mg (63%), blue powder. ¹H NMR (300 MHz, CD₂Cl₂): δ 1.25 (tt, 12H, ³J_{HH} = 7.2 Hz, ³J_{NH} = 1.7 Hz, CH₃CH₂N), 1.96, 2.06, 2.45 (3 \times s, 3 \times 6H, CH₃), 3.21 (q, 8H, ³J_{HH} = 7.3 Hz, CH₃CH₂N), 6.98–7.10 (m, 6H, C_{arom}H). ¹³C NMR (75 MHz, CD₂Cl₂): δ 7.9 (CH₃CH₂N), 18.5, 19.3, 20.6 (CH₃), 53.1 (t, ¹J_{CN} = 3 Hz, CH₃CH₂N), 124.8, 128.1, 128.47, 128.53, 131.0, 151.7 (C_{arom}), 165.7 (C=N). IR (neat): ν 2946 (w), 1895 (m), 1799 (s), 1774 (vs), 1535 (w), 1482 (w), 1441 (w), 1386 (m), 1313 (m), 1258 (w), 1215 (m), 1170 (w), 1093 (w), 975 (m), 846 (m), 785 (m), 702 (m), 629 (m), 617 (w), 564 (w), 547 (w), 470 (w), 434 (w), 417 (m) cm⁻¹.

$(\text{NEt}_4)[\text{Mo}(\text{DAD})(\text{CO})_3\text{Br}]$ (**15**), $(\text{NEt}_4)[\text{Mo}(\text{DAD})(\text{CO})_3\text{I}]$ (**16**), $(\text{NEt}_4)[\text{Mo}(\text{DAD})(\text{CO})_3(\text{NCS})]$ (**17**), $(\text{PPh}_4)[\text{Mo}(\text{DAD})(\text{CO})_3(\text{N}_3)]$ (**20**), $(\text{PPh}_4)[\{\text{Mo}(\text{DAD})(\text{CO})_3\}_2(\mu\text{-N}_3)]$ (**21**), and $(\text{NEt}_4)[\{\text{Mo}(\text{DAD})(\text{CO})_3\}_2(\mu\text{-OAc})]$ (**22**) were obtained using the same protocol; see the SI.

$[\text{Mo}(\text{DAD})(\text{CO})_3(\text{tBuNC})]$ (**12**; *Method D*). **2** (203 mg, 0.40 mmol, 1.00 equiv) was suspended in toluene (15 mL). *tert*-Butylisocyanide (35 mg, 0.42 mmol, 1.05 equiv) was added to the dark-blue mixture. After stirring for 30 min, the precipitated product was isolated by filtration and dried in vacuo. Yield: 162 mg (74%), microcrystalline, dark-blue powder. ¹H NMR (300 MHz, CD₂Cl₂): δ 1.41 (s, 9H, (CH₃)₃CNC), 1.99 (s, 6H, CH₃), 2.18 (s, 12H, CH₃), 7.07–7.19 (m, 6H, C_{arom}H). ¹³C NMR (75 MHz, CD₂Cl₂): δ 18.7, 18.9 (CH₃), 30.7 ((CH₃)₃CNC), 56.8 (t, ¹J_{CN} = 4 Hz, (CH₃)₃CNC), 125.4, 128.3, 128.8, 150.9 (C_{arom}), 164.8 (C=N). IR (neat): ν 2988 (w), 2112 (m), 1912 (s), 1838 (s), 1813 (vs), 1555 (w), 1458 (m), 1370 (w), 1325 (m), 1218 (m), 1194 (w), 1162 (w), 1093 (w), 1035 (m), 849 (w), 769 (s), 701 (w), 630 (w), 585 (w), 521 (m), 492 (w), 446 (m), 421 (m) cm⁻¹.

$[\text{Mo}(\text{DAD})(\text{CO})_3(\text{Im}^{\text{H}})]$ (**10**; Im^H = imidazole), $[\text{Mo}(\text{DAD})(\text{CO})_3(\text{Im}^{\text{I}})]$ (**11**; Im^I = *N*-methylimidazole), and $[\text{Mo}(\text{DAD})(\text{CO})_3(\text{nBu}_3\text{P})]$ (**13**) were obtained according to the same protocol; see the SI.

$(\text{NEt}_4)[\text{Mo}(\text{DAD})(\text{CO})_3(\text{CN})]$ (**18**; *Method E*). A mixture of **2** (114 mg, 0.22 mmol, 1.00 equiv) and NEt₄CN (46 mg, 0.29 mmol, 1.32 equiv) was dissolved in methanol (15 mL). After stirring overnight, the product was precipitated by the addition of diethyl ether (30 mL), isolated by filtration, and dried in vacuo. Yield: 50 mg (36%), microcrystalline, violet powder. ¹H NMR (300 MHz, CD₂Cl₂): δ 1.25 (tt, 12H, ³J_{HH} = 7.3 Hz, ³J_{NH} = 1.8 Hz, CH₃CH₂N), 1.91 (s, 6H, CH₃), 2.24 (br s, 12H, CH₃), 3.20 (q, 8H, ³J_{HH} = 7.3 Hz, CH₃CH₂N), 6.99–7.12 (m, 6H, C_{arom}H). ¹³C NMR (75 MHz, CD₂Cl₂): δ 7.9 (CH₃CH₂N), 18.4 (CH₃), 19.1 (br, CH₃), 53.1 (t, ¹J_{CN} = 3 Hz, CH₃CH₂N), 124.5, 128.3, 129.5, 152.3 (C_{arom}), 161.0 (C=N). IR (neat): ν 2981 (w), 2078 (w), 1899 (s), 1797 (vs), 1589 (w), 1531 (w), 1480 (m), 1438 (m), 1387 (s), 1319 (s), 1258 (w), 1216 (m), 1170 (m), 1157 (w), 1092 (w), 976 (m), 848 (m), 792 (s), 703 (m), 624 (m), 591 (w), 561 (w), 547 (w), 516 (w), 496 (m), 438 (m), 424 (m) cm⁻¹.

$(\text{NEt}_4)[\{\text{Mo}(\text{DAD})(\text{CO})_3\}_2(\mu\text{-CN})]$ (**19**) was obtained using the same protocol; see the SI.

UV/Vis Measurements. Instrumentation and experimental results are given in the SI.

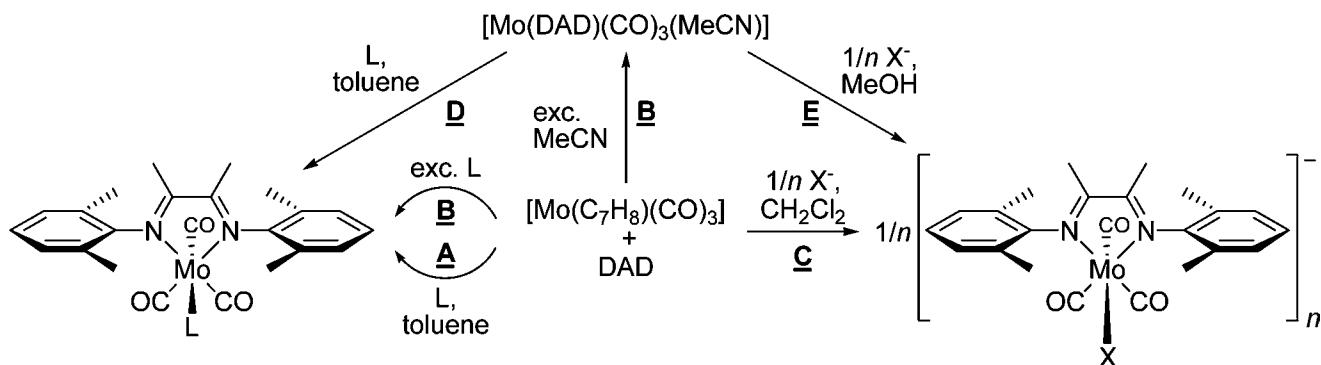
Single-Crystal XRD Studies. Crystallographic details are available in the SI, including ORTEP-style figures, crystal parameters, and data collection and refinement results for all compounds studied by XRD.

All ORTEP-style figures are shown for 50% probability; carbon-bound hydrogen atoms as well as solvent molecules and cations are omitted for clarity.

RESULTS AND DISCUSSION

Syntheses and Reactivities. Molybdenum(0) diazadiene tricarbonyl complexes with phosphanes as coligands have been prepared by thermal displacement of one carbonyl ligand from the corresponding tetracarbonyl complexes.^{14b} However, this method seems unsuitable for thermally less robust products and ligands that are considerably weaker than carbon monoxide. Therefore, substitution of labile ligands at ambient temperature was chosen as a synthetic concept (Scheme 1).^{12a,13a,14b}

Scheme 1. Synthetic Procedures Using Methods A–E



A: L = DMSO **5**, DMF **6**, THT **9**

B: L = MeCN **2**, MeOH **3**, THF **4**, Me₂CO **7**, EtOAc **8**

D: L = Im^H **10**, Im¹ **11**, *t*BuNC **12**, *n*Bu₃P **13**

C, n = 1: X⁻ = Cl⁻ **14**, Br⁻ **15**, I⁻ **16**, NCS⁻ **17**, N₃⁻ **20**

n = 2: μ-X⁻ = μ-N₃⁻ **21**, μ-OAc⁻ **22**

E, n = 1: X⁻ = CN⁻ **18**

n = 2: μ-X⁻ = μ-CN⁻ **19**

Most complexes were prepared by the reaction of molybdenum cycloheptatriene tricarbonyl, [Mo(C₇H₈)(CO)₃], with 1 equiv of DAD and the desired coligand L or X⁻, similar to the corresponding phen and bipy complexes.^{12a,13a} While weakly donating and/or hard ligands were applied in large excess, i.e., as solvents of the reaction (method B), 1 equiv of the stronger donating ligands DMSO, *N,N*-dimethylformamide (DMF), and THT in a toluene solution was sufficient for complete conversion (method A). Anionic coligands X⁻ were introduced as tetraethylammonium salts (tetraphenylphosphonium in the case of azide) using a similar procedure (method C). Dichloromethane was found to be a reasonable compromise between the solubility of the (ionic) starting materials and products, stability of the products, and coordination behavior of the solvent. It was also used for NMR measurements (*vide infra*).

For the ligands with the highest affinity toward molybdenum(0), overreaction was sometimes observed, yielding products not containing any DAD ligands. IR spectra indicated the formation of [Mo(CO)₃L₃] in these cases.²² To overcome this problem, **2** was used as a precursor, giving good yields of the desired complexes (methods D and E).

While the halide anions were found to act exclusively as monodentate ligands toward the complex fragment [Mo(DAD)(CO)₃], different reactivities were observed for the multiaatomic pseudohalides CN⁻, SCN⁻, and N₃⁻ as well as for OAc⁻. These anions are capable of bridging two Mo centers; pure samples of such binuclear complexes were obtained for CN⁻, N₃⁻, and OAc⁻ using the same synthetic protocols as those mentioned above except for the necessarily different stoichiometry. In the case of OAc⁻, only the binuclear complex could be obtained, while for CN⁻ and N₃⁻, both mono- and dinuclear complexes could be prepared selectively.

All complexes were obtained as blue-to-violet, sometimes almost black, microcrystals or powders that give intensely blue-colored solutions. While complexes bearing strong donor/acceptor coligands such as *n*Bu₃P or *t*BuNC are moderately stable toward oxygen both in solution and in the solid state, those compounds with weakly bound coligands such as EtOAc or iodide readily decompose upon contact with air. Slow degradation is also observed in a dichloromethane solution. The tetracarbonyl complex **1** was found to be the dominating decomposition product, presumably formed by CO release from an oxidized tricarbonyl complex and

subsequent ligand exchange on further tricarbonyl complex molecules.

Polarity Measurements. A range of 22 solvents, including 7 room temperature ILs (RTILs), was used to determine the solvatochromic behavior of **1** and the complex fragment [Mo(DAD)(CO)₃]. Complex **1** shows strong negative solvatochromism concerning its MLCT band, similar to a variety of molybdenum(0) diaza ligand tetracarbonyl compounds known in the literature.⁵ **2** was used as the second probe molecule, showing significantly smaller differences in its MLCT band. As expected, donor solvents (L) show the same visible spectra for any labile complex fragment source applied (**2**, [Mo(DAD)(CO)₃L], [Mo(C₇H₈)(CO)₃] + DAD). The triene and free DAD do not interfere because their absorption maxima lie at significantly higher energies compared to the complexes under investigation. The results suggest that ligand-exchange reactions lead to the quantitative *in situ* formation of [Mo(DAD)(CO)₃L] due to fast equilibration. This conclusion is consistent with NMR spectra recorded in acetonitrile showing complete conversion toward the acetonitrile complex **2** upon dissolution of compounds with weak or hard donor ligands, e.g., acetone, EtOAc, and methanol.

In order to clarify the nature of the observed solvatochromic effects, regression analyses were performed against the simplified linear solvation energy relationship of Kamlet et al.²³

$$\nu(\text{probe}) = \nu_0 + a\alpha + b\beta + s\pi^*$$

The solvent parameters α , β , and π^* in this model correspond to the solvent's ability to donate hydrogen bonds (α , acidity) and to accept hydrogen bonds (β , basicity) and to its overall dipolarity and polarizability (π^*). The solvent-independent, solute-characteristic coefficients a , b , and s describe the degree to which the corresponding solvent parameter affects the chromophore's absorption band $\nu(\text{probe})$. Of special interest is the strength of correlation with each parameter that can be quantified as the ratio of the corresponding coefficient and its error.

As can be seen from Table 1, the tetracarbonyl complex **1** shows significant correlation with π^* because of its large value and small relative error of s . While the dependence on α and β is comparably small, the coefficient of determination seems reasonable, leading to the conclusion that the observed MLCT band can be approximated as a function of π^* alone, as shown in Figure 1.

Table 1. Linear Regression Results

[Mo(DAD)(CO) ₄] (1; n = 22; R ² = 0.813)				
	ν_0	a	b	s
coefficient	16918	187	656	1856
error	222	237	286	293
coefficient/error	76.3	0.8	2.3	6.3
[Mo(DAD)(CO) ₃ (MeCN)] (2; n = 18; R ² = 0.567)				
	ν_0	a	b	s
coefficient	15514	153	-799	619
error	281	205	259	329
coefficient/error	55.3	0.7	3.1	1.9

A similar, roughly linear correlation has already been observed for a related molybdenum(0) iminopyridine tetracarbonyl complex and Reichardt's E^T scale.^{6a} Because of the fact that this parameter is, in turn, strongly correlated with π^* for all solvents with low acidity α ,²⁴ this result meets the expectations. Figure 1 also shows

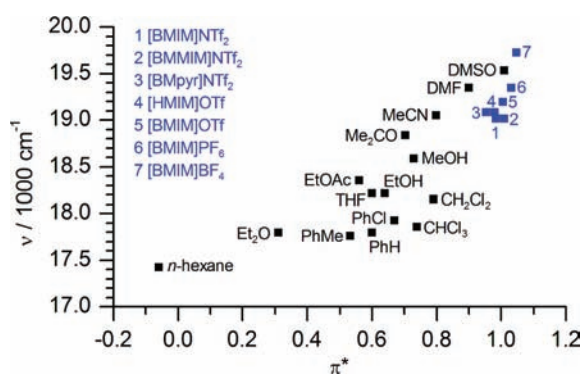


Figure 1. Maximum absorption energy $\nu(1)$ as a function of π^* . Conventional solvents are shown in black and ILs in blue. Data are given in tabular form in the SI. Notation: [BMIM]⁺, 1-butyl-3-methylimidazolium; [BMMIM]⁺, 1-butyl-2,3-dimethylimidazolium; [BMpyr]⁺, 1-butyl-1-methylpyrrolidinium; [HMIM]⁺, 1-hexyl-3-methylimidazolium.

that the used ILs all have π^* values around 1.0 and thus similar absorption bands for **1**.

While the behavior of **1** is consistent with the prediction, the complex fragment [Mo(DAD)(CO)₃] exhibits complicated UV/vis behavior. As stated above, all experimental evidence leads to the conclusion that, in donor solvents L, [Mo(DAD)(CO)₃L] is quantitatively formed. On the other hand, the linear regression shows no strong correlation with any of the Kamlet–Taft parameters (cf. Table 1). This failure of the tested complex fragment as a solvatochromic probe intrigued us and led us to investigate the solution and solid-state properties of the tricarbonyl complexes in some detail.

NMR Spectroscopy. The only (affordable) NMR solvent with sufficient solubilization for a broad range of neutral as well as anionic tricarbonyl complexes was found to be dichloromethane. While donor solvents lead to ligand-exchange reactions and are only suitable for indirect complex characterization, nonpolar solvents do not dissolve most of the complexes, especially in the case of salt-like substances. However, the stability of the tricarbonyl complexes in dichloromethane is limited so that spectra had to be recorded within a couple of hours. Some complexes with weakly bound ligands (acetone, EtOAc, THF, and MeOH) could only be characterized indirectly via NMR spectroscopy using acetonitrile. In these cases, the free coligand and in situ formed acetonitrile complex **2** are found in the correct ratio.

All spectra reveal C_s symmetry for the complex molecules, as expected for the *fac* isomer. Thus, three methyl group signals of equal intensity are usually found in the ¹H NMR spectra. While the carbonyl ligands are mostly not observed because of solubility limitations, the quaternary carbon signals C_{imine} and C_{ipso} are found to be strongly dependent on the coligand L or X⁻. These signals correspond to the two DAD carbon atoms directly bound to the ligating nitrogen atoms and are thus strongly influenced by the metal environment. When any two complexes are compared, it becomes evident that, as the imine resonance is shifted downfield, the aromatic ipso signal is invariably shifted upfield. The relative shift difference $\Delta\delta = \delta(C_{\text{imine}}) - \delta(C_{\text{ipso}})$ of these two signals can therefore be used as a quantitative measure for the ligand's electronic properties.

When the shift differences $\Delta\delta$ of the halide and nonbridged pseudohalide complexes are sorted by increasing values, the same order as that in the spectrochemical series²⁵ is observed for all of these anionic ligands but cyanide (cf. Table 2).

Table 2. Selected Spectroscopic and Solid-State Parameters

compound	coligand	$\Delta\delta/\text{ppm}$	N–Mo–L ^a /deg	Mo–L/pm	$\nu_1(\text{CO})^b/\text{cm}^{-1}$
18	CN ⁻	8.69	c	c	1899
19	$\mu\text{-CN}^-$	8.90	90.3	218.8(3)	1909
16	I ⁻	9.99	c	c	1905
13	<i>n</i> Bu ₃ P	10.17	106.7	257.5(2)	1915
15	Br ⁻	12.76	91.8	273.0(2)	1895
19	$\mu\text{-CN}^-$	13.24	88.4	220.8(3)	1909
12	<i>t</i> BuNC	13.89	91.1	214.8(5)	1912
14	Cl ⁻	14.05	90.9	259.6(2)	1895
10	Im ^H	14.22	88.1	227.0(4)	1895
11	Im ^I	14.30	89.2	228.7(2)	1896
21	$\mu\text{-N}_3^-$	15.28	c	c	1895
20	N ₃ ⁻	15.60	c	c	1888
9	THT	15.98	92.0	261.7(1)	1897
17	NCS ⁻	16.42	87.7	220.8(3)	1884
2	MeCN	17.19	84.7	223.3(3)	1903
22	$\mu\text{-OAc}^-$	17.77	80.6	224.2(3)	1887
			83.4	221.8(4)	
6	DMF	19.12	82.6	224.9(2)	1893
1	CO	19.74	99.1	201.8(2)	1993
			96.9	204.4(2)	2006
			95.4	204.0(4)	
			96.5	203.6(4)	
5	DMSO	19.93	80.5	226.6(2)	1890
4	THF	c	88.7	231.9(3)	1902
3	MeOH	c	82.3	226.8(6)	1895
7	Me ₂ CO	c	80.0	226.6(5)	1893
8	EtOAc	c	76.7	228.5(2)	1896

^aAverage angle between the imine nitrogen, molybdenum, and coligand. ^bHigh-energy CO stretching band. ^cNo value available.

These ligands do not participate in significant π -back-bonding; in fact, the heavier halides are even known to be π donors. The observed trend can thus be readily explained: Coordination of a weaker (stronger π -donating) ligand leads to an accumulation of the electron density at the metal, which, in turn, causes stronger back-bonding to the DAD ligand. The latter can be observed as an upfield shift of the imine carbon resonance, leading to a small $\Delta\delta$.

Table 2 also shows that this concept does not hold for ligands with π -accepting properties like cyanide, tri-*n*-butylphosphine,

DMF, or DMSO. While the former two exhibit unexpectedly small $\Delta\delta$ values, the latter two lead to a DAD ligand with electronic characteristics similar to those in the tetracarbonyl complex. This effect is indicative of some influence of a different nature than pure ligand-field splitting.

IR Spectroscopy. All tricarbonyl complexes show two strong CO stretching vibrations attributed to the symmetry species A_1 and E_1 , as expected for a *fac*-[M(CO)₃L₂L'] complex of local pseudo- C_{3v} symmetry.^{12a,26} As this approximation gets less accurate, e.g., when going from the light halide Cl⁻ to the heavy halide I⁻, the band of lower energy (E_1) progressively splits, leading to three well-separated bands for **16**. A comparison of the high-energy band ν_1 (A_1) with the results from NMR measurements shows similar characteristics: While the observed values of the nonbridging (pseudo)halides except cyanide are consistent with the spectrochemical series, this concept fails for π -accepting ligands.

In general, the differences in the CO bands between different complexes are relatively small and presumably affected by packing effects in the solid state, as suggested by the two different modifications of the tetracarbonyl complex **1** that show different CO bands in the solid state. These findings render IR spectroscopy less helpful in understanding the bonding situation in this class of compounds. However, the clearly separated band of **1**, which is the main contamination arising from decomposition (*vide supra*), proved to be rather useful in the purity determination of the desired tricarbonyl products.

Crystal Structures. Most complexes could be characterized by single-crystal XRD. In addition to being essential for the current investigation, many of the obtained structures represent the first structurally characterized examples of the coordination of various weakly bound ligands to molybdenum(0).

All complexes exhibit *fac*-oriented carbonyl ligands in a distorted octahedral metal environment, as was already concluded from IR and NMR measurements. In order to compress the amount of data to discuss, a statistical analysis was performed on the data sets,²⁷ yielding the extreme values shown in Table 3.

Table 3. Selected Limiting Bond Lengths and Angles (Different Values within One Structure Are Not Averaged)

bond ^a	min/pm	max/pm	L_{\min}^b	L_{\max}^b
Mo–N	216.0(2)	224.2(2)	μ -CN ⁻	CO ^c
Mo–L	201.8(2)	273.0(2)	CO ^c	Br ⁻
Mo–C _{trans}	190.6(9)	198.0(3)	MeOH	μ -CN ⁻
Mo–C _{cis}	189.2(6)	204.4(2)	μ -OAc ⁻	CO ^c
N–C _{imine}	128.7(6)	132.6(7)	μ -OAc ⁻	μ -OAc ⁻
C _{imine} –C _{imine}	144.0(7)	149.0(3)	<i>n</i> Bu ₃ P	EtOAc
N–C _{ipso}	143.4(8)	146.5(11)	<i>n</i> Bu ₃ P	MeOH
angle ^a	min/deg	max/deg	L_{\min}^b	L_{\max}^b
N–Mo–N	71.0(1)	72.4(1)	CO ^d	EtOAc
N–Mo–L	76.7(1)	110.2(2)	EtOAc	<i>n</i> Bu ₃ P
N–Mo–C _{trans}	93.6(2)	103.2(1)	THF	MeCN
N–Mo–C _{cis}	91.7(1)	102.1(1)	CO ^d	μ -CN ⁻
L–Mo–C _{trans}	78.2(2)	99.8(1)	<i>n</i> Bu ₃ P	EtOAc
Mo–N–C _{imine}	116.2(2)	120.2(2)	DMSO	<i>t</i> BuNC
Mo–N–C _{ipso}	119.9(1)	125.8(4)	CO ^c	Me ₂ CO

^aNotation: N, imine nitrogen; L, coligand (regardless of charge); C_{cis}/C_{trans}, carbonyl carbon in *cis/trans* position to DAD. ^bColigand that corresponds to the structure with smallest (L_{\min}) or largest (L_{\max}) value observed. ^cFirst modification. ^dSecond modification.

It is evident that the various complexes differ significantly in their geometric arrangement directly at the molybdenum atom,

while the DAD moiety undergoes minor changes in the bond lengths and angles. The bite angle N–Mo–N remains almost constant at 71–72°, while the bond length Mo–N varies between 216 and 224 pm. Most interesting is the angle N–Mo–L between DAD and the coligand, which varies greatly from 76.7° to 110.2° and will be discussed in detail (*vide infra*). Because of the different ligating atoms, the distances Mo–L also differ strongly. These mostly unprecedented bond lengths are tabulated in Table 2, hopefully providing a useful source of information for comparison with other zerovalent molybdenum compounds in the future.

The bond length Mo–P in **13** [257.5(2) pm] is consistent with those found for other molybdenum tricarbonyl complexes ([Mo(bipy)(CO)₃(PPh₃)], Mo–P = 260.3(1) pm;^{17d} [Mo(phen)(CO)₃(PPh₃)], Mo–P = 259.7(1) pm;^{17c} [Mo(phen)(CO)₃(η^1 -dppm)] [dppm = 1,1-bis(diphenylphosphino)methane], Mo–P = 257.2(3) pm;^{17a} [Mo(PyCa^{OH})(CO)₃(PPh₃)] (PyCa^{OH} = 4-hydroxyphenyl-pyridine-2-carbaldimine), Mo–P = 257.0(1) pm;^{17b} [Mo(PyCa^{OH})(CO)₃(PPh₃)·Et₂O], Mo–P = 253.3(1) pm^{17b}). However, all of the known structures show angles N–Mo–P in the range of 85.5(2)–92.3(6)°, which deviates substantially from the averaged value found for **13** (106.7°), most likely because of steric reasons (*vide infra*). Similarly, the bond lengths Mo–L [**4**, L = THF, Mo–O = 231.9(3) pm; **10**, L = Im^H, Mo–N = 227.0(4) pm; **11**, L = Im^L, Mo–N = 228.7(2) pm; **12**, L = *t*BuNC, Mo–C = 214.8(5) pm] are found to compare well with reported values [[Mo(PyCa^{OH})(CO)₃(THF)], Mo–O = 228.9(3) pm;^{17b} [Mo(bipy)(CO)₃(py)], Mo–N = 231.1(9) pm;^{18a} [Mo(bipy)(CO)₃(η^1 -dipyam)] [dipyam = *N,N*-bis(2-pyridyl)amine], Mo–N = 235.2(6) pm;^{18b} [Mo(PyCa^{OH})(CO)₃(*t*BuNC)], Mo–C = 216.6(3) pm;^{17b} [Mo(PyCa^{OH})(CO)₃(CyNC)], Mo–C = 215.1(2) pm^{17b}], while the angles N–Mo–L seem to strongly depend on the respective coordination sphere of the metal.

While the different Mo–C distances can be explained by varying back-bonding situations with different coligands, the variation in the bond angles N–Mo–C reflects the distortion caused by different angles N–Mo–L stated above. The DAD moiety exhibits less pronounced structural changes within the expected ranges.²⁸

Figure 2 exemplifies some of the determined structures. While *n*Bu₃P as the coligand leads to a larger angle N–Mo–L, as was expected because of steric hindrance, those complexes with acute angles N–Mo–L, e.g., **5** (L = DMSO, mean value = 80.5°) and **8** (L = EtOAc, mean value = 76.7°), suffer greater steric strain. This is partly released by twisting and/or deflecting the aromatic substituents away from the coligand. In attempts to understand the nature of this obviously electronically induced approach of DAD and the coligand, NMR spectroscopy proves helpful. A comparison of the “irregular” cases, in which $\Delta\delta$ does not allow for the correct placement of the respective coligand in the spectrochemical series (*vide supra*), with the angles N–Mo–L that deviate substantially from 90° shows strong overlap of both categories. Furthermore, a direct correlation between $\Delta\delta$ and N–Mo–L exhibits a smooth trend (Figure 3).

Apparently, a smaller angle N–Mo–L and thereby a greater proximity between the coligand and DAD leads to less electron density in the conjugated C=N double bonds (larger $\Delta\delta$). In fact, the distances between the coligand and imine carbon atoms are unusually small and fall, in part, below the respective van der Waals distances. While theoretical calculations will be necessary to ensure the exact electronic situation, a preliminary interpretation could be as follows: The coligands with the

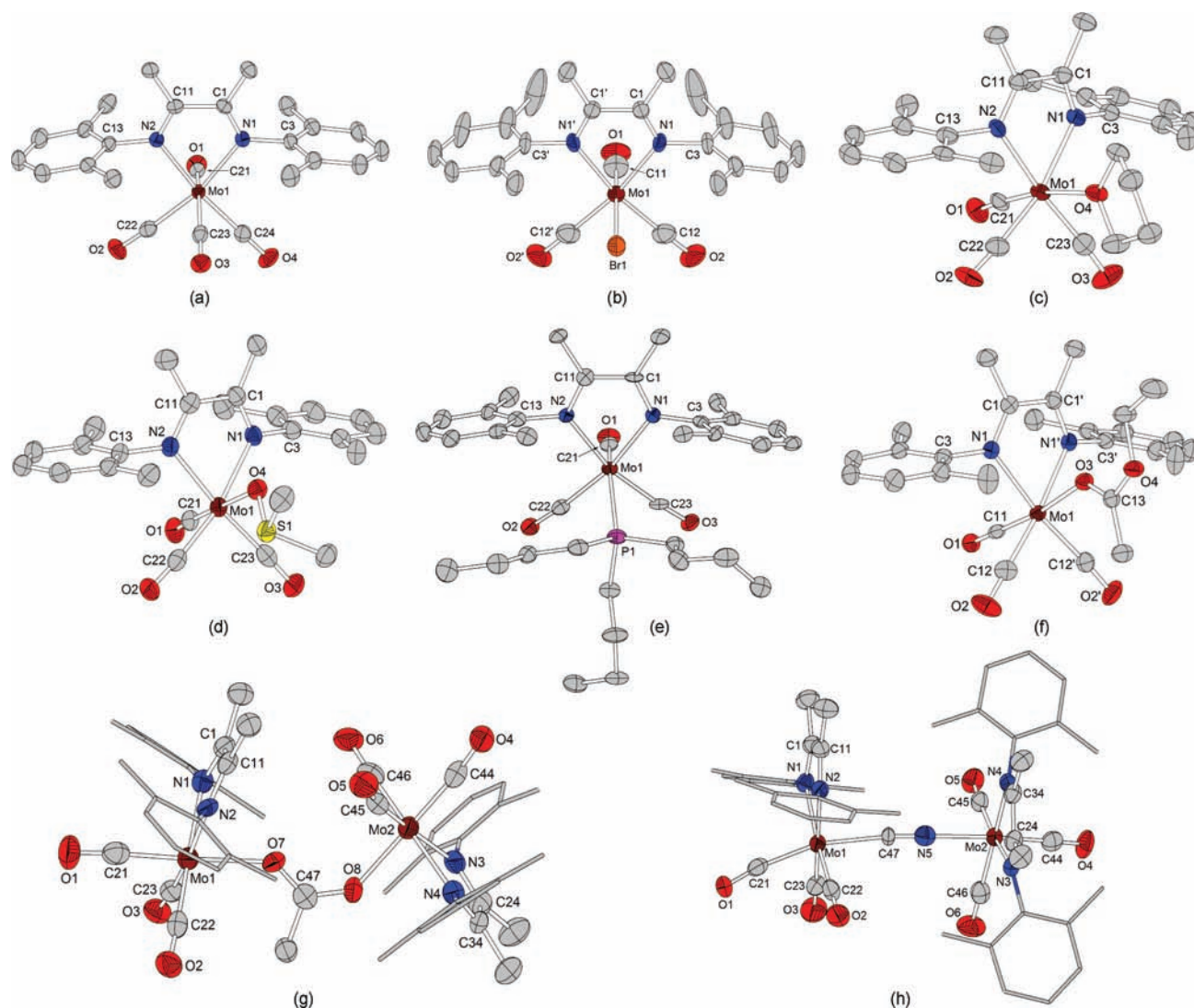


Figure 2. Molecular structures of complexes with weak (upper row) and strong (middle row) deviation from octahedral coordination; dinuclear complexes (lower row): (a) L = CO (1), (b) X⁻ = Br⁻ (15), (c) L = THF (4), (d) L = DMSO (5), (e) L = *n*Bu₃P (13), (f) L = EtOAc (8), (g) μ-X⁻ = μ-OAc⁻ (22), (h) μ-X⁻ = μ-CN⁻ (19).

strongest effect on the angle N–Mo–L (MeCN, μ-OAc⁻, DMF, DMSO, MeOH, Me₂CO, and EtOAc) as well as on Δδ (MeCN, μ-OAc⁻, DMF, and DMSO) all have π* orbitals that point toward the C=N double bonds (cf. Figure 2). The single exception to this rule is methanol, which features an acidic, i.e., electron-poor, proton instead of π* orbitals in the relevant orientation. Because of the short interligand distance, a direct transfer of the electron density from the DAD π orbitals to the coligand seems likely. In other words, an attractive ligand–ligand interaction is proposed that results in the partial displacement of the tricarbonyl complex fragment's back-bonding capacity from the metal to the DAD ligand. A schematic representation of the proposed interaction is shown in Figure 4.

To the best of the authors' knowledge, such an interaction has not been observed for DAD complexes before. In the solid-state structure of [Mo(phen)(CO)₃(SO₂)], Ryan and co-workers²⁰ found the carbonyl ligand in a trans position to sulfur dioxide to be tilted away from phen, resulting in a distortion similar to that in the current investigation. They also postulate this effect to be inherent in such *fac*-tricarbonyl complexes but do not present further details concerning its origin. The high variability of the

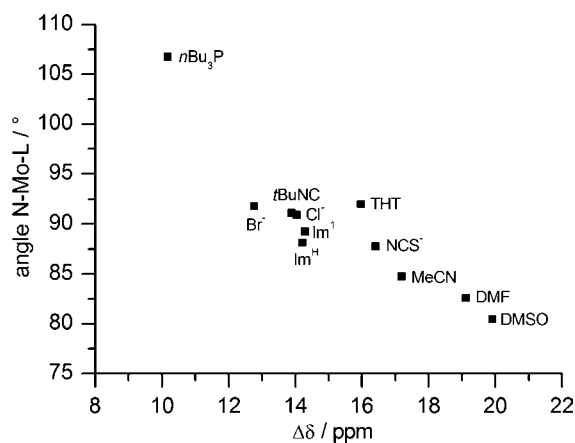


Figure 3. Correlation of the average bond angle N–Mo–L (N–Mo–X for anionic complexes) with Δδ = δ(C_{imine}) – δ(C_{ipso}) for tricarbonyl complexes [Mo(DAD)(CO)₃(L/X)]^{0/-}, as observed by ¹³C NMR.

coligand–molybdenum–carbonyl axis twist leads to the conclusion that the different coligands exert a major influence on this effect.

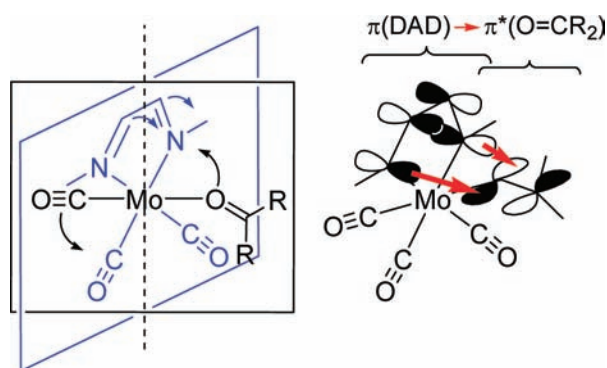


Figure 4. Main observed distortion of the tricarbonyl complexes (left) and the proposed orbital overlap (right) both shown for coligand $O=CR_2$ as a typical example.

However, the donor character of DAD π orbitals has been demonstrated by side-on metal complexes in which six-electron or even eight-electron donation occurs.²⁸ The geometric feasibility of the postulated $\pi(DAD) \rightarrow \pi^*(L)$ orbital overlap is suggested by studies of Stufkens and co-workers^{7b} attributing increased intensity of $\nu(CO_{cis})$ in resonance Raman experiments to a geometrically similar $\pi^*(DAD) \rightarrow \pi^*(CO_{cis})$ overlap.

Interestingly, also the opposite direction of electron transfer, i.e., donation from coligand orbitals into DAD π^* orbitals, has been discussed in terms of theoretical calculations on metal-mediated ester hydrolysis.²⁹ While the model complex $[Mo(HN=CHCH=NH)(CO)_2(\eta^3-C_3H_5)(OH)]$ investigated there features a very electron-poor DAD and the electron-rich, hard coligand hydroxide, the complexes studied here feature an electron-rich DAD because of methyl substitution at the imine carbon atoms. Together with comparably electron-poor coligands like acetone or ethyl acetate, this seemingly leads to an inversion of the respective orbital energies, as suggested by NMR measurements (vide supra).

The failure of the solvatochromic measurements of donor solvents L using in situ generated tricarbonyl complexes $[Mo(DAD)(CO)_3L]$ can be explained by these findings: Variations in the donor/acceptor capabilities of the coligand do change not only the electronic situation at the metal center but also the complex geometry and most likely the strength of ligand–ligand interactions. These effects are dependent on the availability of donor and acceptor orbitals at the solvent's donor functionality. Therefore, a simple correlation with the Kamlet–Taft parameters α , β , or π^* is not possible.

CONCLUSIONS

The current study shows that mixed tricarbonyl DAD complexes of molybdenum(0) are accessible for a wide range of neutral as well as anionic coligands. While the general reactivity of these compounds resembles that of the respective bipy and phen complexes, new insight was gained by extensive structural characterization. Correlation of ^{13}C NMR shifts with structural features of the complexes proved to be a valuable tool for understanding the electronic situation. Thus, we gained structural and spectroscopic evidence for an attractive interaction of DAD and coligands L displaying π^* orbitals such as DMF, DMSO, Me_2CO , EtOAc, and MeCN.

A good correlation of the MLCT absorption band of the tetracarbonyl complex **1** with the Kamlet–Taft polarity parameter π^* is demonstrated for a range of organic solvents including a set of seven ILs. Although the attempted utilization of the tricarbonyl solvent complexes $[Mo(DAD)(CO)_3L]$ as solvatochromic probes was less successful, these compounds, nevertheless, seem to

be a quite interesting class of complexes because the observed DAD–coligand secondary interaction could be useful for activation of the $C=O$ double bonds in catalytic applications.

ASSOCIATED CONTENT

Supporting Information

X-ray crystallographic data in CIF format, listings of known related compounds, full experimental detail and characterization of compounds, details on UV/vis measurements, ORTEP-style plots, and NMR spectra. This material is available free of charge via the Internet at <http://pubs.acs.org>.

AUTHOR INFORMATION

Corresponding Author

*E-mail: jsu@staff.uni-marburg.de. Tel: +49 (0)6421 28-25693. Fax: +49 (0)6421 28-25711.

Notes

The authors declare no competing financial interest.

ACKNOWLEDGMENTS

Routine data collection was performed by the XRD service department (Drs. K. Harms, G. Geiseler, M. Marsch, and R. Riedel) of the Chemistry Department, Philipps University, and is gratefully acknowledged.

REFERENCES

- (1) (a) Bock, H.; tom Dieck, H. *Angew. Chem.* **1966**, *78*, 549–550; *Angew. Chem., Int. Ed. Engl.* **1966**, *5*, 520–522. (b) Bock, H.; tom Dieck, H. *Chem. Ber.* **1967**, *100*, 228–246. (c) tom Dieck, H.; Renk, I. W. *Chem. Ber.* **1971**, *104*, 110–130. (d) Walther, D. *Z. Anorg. Allg. Chem.* **1974**, *405*, 8–18. (e) Majunke, W.; Leibfritz, D.; Mack, T.; tom Dieck, H. *Chem. Ber.* **1975**, *108*, 3025–3029. (f) tom Dieck, H.; Renk, I. W.; Franz, K. D. *J. Organomet. Chem.* **1975**, *94*, 417–424. (g) Walther, D.; Teutsch, M. *Z. Chem.* **1976**, *16*, 118–119. (h) Balk, R. W.; Stufkens, D. J.; Oskam, A. *Inorg. Chim. Acta* **1978**, *28*, 133–143. (i) Staal, L. H.; Terpstra, A.; Stufkens, D. J. *Inorg. Chim. Acta* **1979**, *34*, 97–101. (j) tom Dieck, H.; Mack, T.; Peters, K.; von Schnering, H. G. *Z. Naturforsch. B* **1983**, *38*, 568–579. (k) Herrick, R. S.; Ziegler, C. J.; Bohan, H.; Corey, M.; Eskander, M.; Giguere, J.; McMicken, N.; Wrona, I. E. *J. Organomet. Chem.* **2003**, *687*, 178–184. (2) (a) Stiddard, M. H. B. *J. Chem. Soc.* **1962**, 4712–4715. (b) Graziani, M.; Zingales, F.; Belluco, U. *Inorg. Chem.* **1967**, *6*, 1582–1586. (c) Hutchinson, B.; Nakamoto, K. *Inorg. Chim. Acta* **1969**, *3*, 591–595. (d) tom Dieck, H.; Franz, K.-D.; Hohmann, F. *Chem. Ber.* **1975**, *108*, 163–173. (e) Blandamer, M. J.; Burgess, J.; Chambers, J. G.; Duffield, A. J. *Transition Met. Chem.* **1981**, *6*, 156–163. (f) Connor, J. A.; Overton, C. J. *Organomet. Chem.* **1983**, *249*, 165–174. (g) Herrmann, W. A.; Thiel, W. R.; Kuchler, J. G. *Chem. Ber.* **1990**, *123*, 1953–1961. (h) Herrmann, W. A.; Thiel, W. R.; Kuchler, J. G.; Behm, J.; Herdtweck, E. *Chem. Ber.* **1990**, *123*, 1963–1970. (i) Baxter, P. N. W.; Connor, J. A.; Wallis, J. D.; Povey, D. C.; Powell, A. K. *Polyhedron* **1992**, *11*, 1771–1777. (j) Van Atta, S. L.; Duclos, B. A.; Green, D. B. *Organometallics* **2000**, *19*, 2397–2399. (k) Malkov, A. V.; Baxendale, I. R.; Bella, M.; Langer, V.; Fawcett, J.; Russell, D. R.; Mansfield, D. J.; Valko, M.; Kočovský, P. *Organometallics* **2001**, *20*, 673–690. (l) Zhang, H.; Zhu, C.-F.; Hung, Y.-Q.; Zou, W.; Li, L.; Chen, J.-G.; Gao, J.-X. *Xiamen Daxue Xuebao, Ziran Kexueban Bianjibu* **2004**, *43*, 71–76. (m) Ardon, M.; Hogarth, G.; Oscroft, D. T. W. *J. Organomet. Chem.* **2004**, *689*, 2429–2435. (n) Braga, S. S.; Coelho, A. C.; Gonçalves, I. S.; Almeida Paz, F. A. *Acta Crystallogr., Sect. E* **2007**, *63*, m780–m782. (3) (a) Hieber, W.; Mühlbauer, F. *Z. Anorg. Allg. Chem.* **1935**, *221*, 337–348. (b) Graham, J. R.; Angelici, R. J. *Inorg. Chem.* **1967**, *6*, 992–998. (c) Dobson, G. R.; Asali, K. J. *Inorg. Chem.* **1981**, *20*, 3563–3564. (d) Slot, H. J. B.; Murrall, N. W.; Welch, A. J. *Acta Crystallogr., Sect. C* **1985**, *41*, 1309–1312. (e) Sjögren, M. P. T.; Frisell, H.; Åkermark, B.;

- Norrby, P.-O.; Eriksson, L.; Vitagliano, A. *Organometallics* **1997**, *16*, 942–950. (f) Xie, X. J.; Jin, X. L.; Tang, K. L. *Acta Crystallogr., Sect. C* **2001**, *57*, 696–697. (g) Yang, L.; Feng, J.-K.; Ren, A.-M. *Synth. Met.* **2005**, *152*, 265–268.
- (4) (a) Brunner, H.; Herrmann, W. A. *Chem. Ber.* **1972**, *105*, 770–783. (b) Walther, D. Z. *Anorg. Allg. Chem.* **1973**, *396*, 46–58. (c) Alyea, E. C.; Jain, V. K. *Polyhedron* **1996**, *15*, 1723–1730. (d) Mentes, A. *Transition Met. Chem.* **1999**, *24*, 77–80. (e) Herrick, R. S.; Houde, K. L.; McDowell, J. S.; Kiczek, L. P.; Bonavia, G. *J. Organomet. Chem.* **1999**, *589*, 29–37. (f) Burgess, J.; Fawcett, J.; Russell, D. R.; Sawbridge, J.; Vu, H. *Transition Met. Chem.* **2000**, *25*, 547–551. (g) Gilani, S. R.; Mahmood, Z. *J. Chem. Soc. Pak.* **2003**, *25*, 41–43. (h) Mentes, A.; Buyukgungor, O. *Acta Crystallogr., Sect. E* **2004**, *60*, m530–m531. (i) Ederer, T.; Herrick, R. S.; Beck, W. Z. *Anorg. Allg. Chem.* **2006**, *633*, 235–238. (j) García-Rodríguez, R.; Miguel, D. *Dalton Trans.* **2006**, 1218–1225. (k) Datta, P.; Sinha, C. *Polyhedron* **2007**, *26*, 2433–2439. (l) Karakus, M.; Davulga, G.; Gómez-Ruiz, S.; Tschirschwitz, S.; Hey-Hawkins, E. *Polyhedron* **2009**, *28*, 91–94. (m) Álvarez, C. M.; García-Rodríguez, R.; Martín-Alvarez, J. M.; Miguel, D. *Dalton Trans.* **2010**, 39, 1201–1203.
- (5) (a) Burgess, J. *J. Organomet. Chem.* **1969**, *19*, 218–220. (b) tom Dieck, H.; Renk, I. W. *Angew. Chem.* **1970**, *82*, 805–807; *Angew. Chem., Int. Ed. Engl.* **1970**, *9*, 793–795. (c) Burgess, J.; Morton, S. F. N. *J. Chem. Soc., Dalton Trans.* **1972**, 1712–1714. (d) Connor, J. A.; Overton, C.; El Murr, N. *J. Organomet. Chem.* **1984**, *277*, 277–284. (e) Macholdt, H.-T.; van Eldik, R.; Kelm, H. *Inorg. Chim. Acta* **1985**, *104*, 115–118. (f) bin Ali, R.; Burgess, J.; Kotowski, M.; van Eldik, R. *Transition Met. Chem.* **1987**, *12*, 230–235. (g) bin Ali, R.; Burgess, J. *Transition Met. Chem.* **1993**, *18*, 9–18. (h) Baxter, P. N. W.; Connor, J. A. *J. Organomet. Chem.* **1995**, *486*, 115–121. (i) Burgess, J.; Maguire, S.; McGranaghan, A.; Parsons, S. A.; Nowicka, B.; Samotus, A. *Transition Met. Chem.* **1998**, *23*, 615–618.
- (6) (a) Walther, D. *J. Prakt. Chem.* **1974**, *316*, 604–614. (b) Burgess, J.; Chambers, J. G.; Haines, R. I. *Transition Met. Chem.* **1981**, *6*, 145–151. (c) Manuta, D. M.; Lees, A. J. *Inorg. Chem.* **1983**, *22*, 3825–3828. (d) George, J. E.; Drago, R. S. *Inorg. Chem.* **1996**, *35*, 239–241.
- (7) (a) Wrighton, M. S.; Morse, D. L. *J. Organomet. Chem.* **1975**, *97*, 405–420. (b) Staal, L. H.; Stufkens, D. J.; Oskam, A. *Inorg. Chim. Acta* **1978**, *26*, 255–262. (c) Balk, R. W.; Stufkens, D. J.; Oskam, A. *Inorg. Chim. Acta* **1979**, *34*, 267–274. (d) Balk, R. W.; Snoeck, T.; Stufkens, D. J.; Oskam, A. *Inorg. Chem.* **1980**, *19*, 3015–3021. (e) Manuta, D. M.; Lees, A. J. *Inorg. Chem.* **1986**, *25*, 1354–1359. (f) Kalyanasundaram, K. *J. Phys. Chem.* **1988**, *92*, 2219–2223. (g) Rawlins, K. A.; Lees, A. J. *Inorg. Chem.* **1989**, *28*, 2154–2160. (h) Schneider, K. J.; van Eldik, R. *Organometallics* **1990**, *9*, 92–96. (i) Wieland, S.; Reddy, K. B.; van Eldik, R. *Organometallics* **1990**, *9*, 1802–1806. (j) Stufkens, D. J.; Oskam, A. *J. Mol. Struct.* **1990**, *217*, 131–142. (k) Fu, W.-F.; van Eldik, R. *Inorg. Chem.* **1998**, *34*, 1044–1050.
- (8) (a) Haga, M.-A.; Koizumi, K. *Inorg. Chim. Acta* **1985**, *104*, 47–50. (b) Baxter, P. N. W.; Connor, J. A. *J. Organomet. Chem.* **1988**, *355*, 193–196. (c) Bildstein, B.; Malaun, M.; Kopacka, H.; Fontani, M.; Zanello, P. *Inorg. Chim. Acta* **2000**, *300–302*, 16–22. (d) Wuckelt, J.; Döring, M.; Görls, H.; Langer, P. *Eur. J. Inorg. Chem.* **2001**, 805–811. (e) Heinze, K.; Toro, J. D. B. *Angew. Chem., Int. Ed.* **2003**, *42*, 4533–4536. (f) Heinze, K.; Jacob, V. *Eur. J. Inorg. Chem.* **2003**, 3918–3923. (g) Paul, F.; Goeb, S.; Justaud, F.; Argouarch, G.; Toupet, L.; Ziessel, R. F.; Lapinte, C. *Inorg. Chem.* **2007**, *46*, 9036–9038. (h) Packheiser, R.; Ecorchard, P.; Rüffer, T.; Walfort, B.; Lang, H. *Eur. J. Inorg. Chem.* **2008**, *26*, 4152–4165.
- (9) (a) Dessy, R. E.; Pohl, R. L. *J. Am. Chem. Soc.* **1968**, *90*, 2005–2008. (b) Dessy, R. E.; Charkoudian, J. C.; Abeles, T. P.; Rheingold, A. L. *J. Am. Chem. Soc.* **1970**, *92*, 3947–3956. (c) tom Dieck, H.; Kuehl, E. Z. *Naturforsch. B* **1982**, *37*, 324–331. (d) Miholová, D.; Gaš, B.; Zališ, S.; Klíma, J.; Vlček, A. A. *J. Organomet. Chem.* **1987**, *330*, 75–84. (e) Hanzlík, J.; Pospíšil, L.; Vlček, A. A.; Krejčík, M. *J. Elektroanal. Chem.* **1992**, *331*, 831–844. (f) Johnson, R.; Madhani, H.; Bullock, J. P. *Inorg. Chim. Acta* **2007**, *360*, 3414–3423.
- (10) (a) Mentes, A.; Sarbay, M.; Hazer, B.; Arslan, H. *Appl. Organomet. Chem.* **2005**, *19*, 76–80. (b) Mentes, A.; Hanhan, M. E. *Transition Met. Chem.* **2008**, *33*, 91–97.
- (11) (a) Stiddard, M. H. B. *J. Chem. Soc.* **1963**, 756–757. (b) Graham, J. R.; Angelici, R. J. *J. Am. Chem. Soc.* **1965**, *87*, 5590–5597. (c) Houk, L. W.; Dobson, G. R. *J. Chem. Soc. A* **1966**, 317–319. (d) Houk, L. W.; Dobson, G. R. *Inorg. Chem.* **1966**, *5*, 2119–2123. (e) Dalton, J.; Paul, I.; Smith, J. G.; Stone, F. G. A. *J. Chem. Soc. A* **1968**, 1208–1211. (f) Angelici, R. J.; Jacobson, S. E.; Ingemanson, C. M. *Inorg. Chem.* **1968**, *7*, 2466–2468. (g) Behrens, H.; Lehnert, G.; Sauerborn, H. Z. *Anorg. Allg. Chem.* **1970**, *374*, 310–317. (h) Behrens, H.; Topf, W.; Ellermann, J. *J. Organomet. Chem.* **1973**, *63*, 349–367. (i) Tripathi, S. C.; Srivastava, S. C.; Pandey, R. D.; Mani, R. P. *J. Organomet. Chem.* **1976**, *110*, 67–71. (j) Condon, D.; Deane, M. E.; Lalor, F. J.; Connelly, N. G.; Lewis, A. C. *J. Chem. Soc., Dalton Trans.* **1977**, 925–931. (k) Hor, T. S. A. *Inorg. Chim. Acta* **1987**, *128*, L3–L4. (l) Hor, T. S. A.; Rus, S. R. B. *J. Organomet. Chem.* **1988**, *348*, 343–347. (m) Nakazawa, H.; Ohta, M.; Miyoshi, K.; Yoneda, H. *Organometallics* **1989**, *8*, 638–644. (n) Alyea, E. C.; Gossage, R. A.; Malito, J.; Munir, Z. A. *Polyhedron* **1990**, *9*, 1059–1063. (o) Ocasio-Delgado, Y.; de Jesús-Segarra, J.; Cortés-Figueroa, J. E. *J. Organomet. Chem.* **2005**, *690*, 3366–3372.
- (12) (a) Behrens, H.; Lindner, E.; Lehnert, G. *J. Organomet. Chem.* **1970**, *22*, 439–448. (b) Tripathi, S. C.; Srivastava, S. C. *J. Organomet. Chem.* **1970**, *25*, 193–197. (c) Behrens, H.; Topf, W.; Ellermann, J. *J. Organomet. Chem.* **1973**, *63*, 369–380.
- (13) (a) Behrens, H.; Lindner, E.; Lehnert, G. *J. Organomet. Chem.* **1970**, *22*, 665–676. (b) Brisdon, B. J.; Edwards, D. A.; White, J. W. *J. Organomet. Chem.* **1978**, *156*, 427–437. (c) Sellmann, D.; Weber, W.; Liehr, G.; Beck, H. P. *J. Organomet. Chem.* **1984**, *269*, 155–170.
- (14) (a) Renk, I. W.; tom Dieck, H. *Chem. Ber.* **1972**, *105*, 1403–1418. (b) tom Dieck, H.; Renk, I. W. *Chem. Ber.* **1972**, *105*, 1419–1430.
- (15) (a) Balk, R. W.; Stufkens, D. J.; Oskam, A. *Inorg. Chim. Acta* **1981**, *48*, 105–115. (b) Bell, A.; Walton, R. A. *Polyhedron* **1986**, *5*, 845–858.
- (16) Grevels, F.-W.; Kerpen, K.; Klotzbücher, W. E.; Schaffner, K. *Organometallics* **2001**, *20*, 4775–4792.
- (17) (a) Cano, M.; Campo, J. A.; Pérez-García, V.; Gutiérrez-Puebla, E. *J. Organomet. Chem.* **1990**, *382*, 397–406. (b) Heinze, K. *J. Chem. Soc., Dalton Trans.* **2002**, 540–547. (c) Muir, K. J.; McQuillan, G. P.; Harrison, W. T. A. *Acta Crystallogr., Sect. E* **2007**, *63*, m2492. (d) Muir, K. J.; McQuillan, G. P.; Harrison, W. T. A. *Acta Crystallogr., Sect. E* **2007**, *63*, m2493.
- (18) (a) Griffiths, A. J. *Cryst. Mol. Struct.* **1971**, *1*, 75–82. (b) Howie, R. A.; McQuillan, G. P. *J. Chem. Soc., Dalton Trans.* **1986**, 759–764.
- (19) Heinze, K.; Jacob, V. *J. Chem. Soc., Dalton Trans.* **2002**, 2379–2385.
- (20) Kubas, G. J.; Ryan, R. R.; McCarty, V. *Inorg. Chem.* **1980**, *19*, 3003–3007.
- (21) Oelkers, B.; Sundermeyer, J. *Dalton Trans.* **2011**, *40*, 12727–12741.
- (22) Behrens, H.; Harder, N. *Chem. Ber.* **1964**, *97*, 433–442.
- (23) (a) Kamlet, M. J.; Abboud, J. L.; Taft, R. W. *J. Am. Chem. Soc.* **1977**, *99*, 6027–6038. (b) Kamlet, M. J.; Abboud, J.-L. M.; Abraham, M. H.; Taft, R. W. *J. Org. Chem.* **1983**, *48*, 2877–2887.
- (24) (a) Reichardt, C. *Chem. Rev.* **1994**, *94*, 2319–2358. (b) Reichardt, C. *Green Chem.* **2005**, *7*, 339–351.
- (25) (a) Tsuchida, R. *Bull. Chem. Soc. Jpn.* **1938**, *13*, 388–400. (b) Kettle, S. F. A. *Physical Inorganic Chemistry, A Coordination Chemistry Approach*; Oxford University Press: Oxford, U.K., 1998.
- (26) Hollas, M. J. *Modern Spectroscopy*, 4th ed.; John Wiley & Sons: Chichester, U.K., 2004.
- (27) PreQuest [Cambridge Crystallographic Data Centre (CCDC), **2011**] was used to generate a searchable database from the herein presented XRD data. ConQuest 1.13 (CCDC, **2011**) and Mercury 2.4.5 (CCDC, **2010**) were used for data preparation.
- (28) van Koten, G.; Vrieze, K. *Adv. Organomet. Chem.* **1982**, *21*, 151–239.
- (29) Yeguas, V.; Campomanes, P.; López, R. *Organometallics* **2007**, *26*, 5271–5277.